Novel High-speed State-of-charge Alignment Algorithm for EV Battery Maintenance

Nguyen-Anh Nguyen, Phuong-Ha La, *Student Member, IEEE*, and Sung-Jin Choi, *Member, IEEE*

***Abstract*—For the maintenance of electric vehicle batteries, a special apparatus achieving the state-of-charge (SOC) alignment of the whole cells inside a battery pack is highly promising. Specifically, when battery packs are discharged to a safe SOC level before shipping, according to battery logistic policy, and charged back to a nominal SOC level before being replaced in the swapping station, the SOC levels of all cells should be aligned to a specific target level. Conventionally, numerous cell-balancing hardware architectures and control strategies are studied; however, they only equalize the SOC between cells, and a whole pack SOC alignment feature has not been evaluated. In this paper, a novel algorithm with a coordinated operation between a pack-charger and cell-equalizer is proposed as a viable SOC alignment algorithm. The full-duplex coordinated strategy, which utilizes a bidirectional pack-charger and cell-equalizer, is proposed for alignment purposes, which can minimize the operating time and the energy loss. The theoretical strategy is investigated to achieve the minimal operation time, and the performance of the proposed method is verified by a hardware prototype for a battery pack with 20-series cells. After the alignment process, the cell SOC levels are equalized within a voltage deviation of 30 mV or SOC deviation of 3 %, when the pack SOC level is simultaneously adjusted to a preset level. In comparison with the half-duplex strategy, the proposed strategy has a twice faster processing time, while the energy loss during the process is 38 %, 10.4 % and 26.1 % lower than before. Otherwise, the proposed strategy is achieved higher speed of 52 % and 28.9 % compared with the conventional strategies in balancing speed comparison.**

***Index Terms*—Battery maintenance, battery swapping, charging and equalizing strategy, SOC alignment, full-duplex, charge transfer strategy.**

I. Introduction

ELECTRIC vehicles (EVs) are a promising solution to reduce greenhouse gas emissions; hence, the EV fleet is growing rapidly along with technological development. In addition, the EV battery pack must be retired when its capacity falls below 80 % of the designed level [2] to ensure its operational capability. Thus, it raises future concerns about the disposal of retired battery packs from EVs. According to the International Energy Agency (IEA), the energy of retired EV batteries could reach 120GWh by 2030 [3]. Although battery pack recycling processes have been introduced, the high labor cost limits this as a practical feasibility [4], [5]. From an economic perspective, 80 % of the remaining capacity of the retired battery pack can be reutilized for other purposes such as a battery energy storage system (BESS), or home energy storage, etc. Since the effectiveness of the repurposed battery pack has been verified in terms of economic and environmental analysis [6], [7], battery energy storage systems that utilize reused battery packs are about to gain importance in the marketplace [8]. However, the aging patterns of the cells are known to be different from each other [9]–[11].

Therefore, the EV battery pack requires an innovative and sophisticated maintenance technology. One critical requirement is that the cells inside a battery pack should be maximally balanced as rapidly as possible. For the cell equalization feature, various techniques have been introduced and are classified into four groups based on the charge transfer scheme, as shown in Fig. 1. Meanwhile, the cell-by-adjacent-cell method autonomously exchanges the energy between two adjacent cells using a switched-energy-tank (SET) such as a switched-capacitor [12], [13] or switched-inductor [14], [15]. Hence, the efficiency of the equalizer is high with slightly increased circuit complexity. However, the equalization speed and performance of the equalizer are strongly dependent on the initial voltage distribution of the cells in the series-connected string. By inheriting the advantage of the SET equalizer, a switch-matrix is combined into the structure to form a governed SET equalizer, and thus, energy can be directly transferred from any cell to any cell [16], [17]. By virtue of the switch-matrix, the energy loss during the equalization process is significantly reduced and the dependence on the initial cell voltage distribution is almost eliminated. Furthermore, the isolated converter-based equalizer is adopted to ensure a constant equalization speed. By combining the advantages of the switch-matrix and the isolated converter, the equalizer can achieve a good performance in terms of the degree of

This work was supported by the National Research Foundation of Korea (NRF) grant funded by the Korea government (MSIT) (RS-2023-00240194) and by the Technology Development Program (S3327193) funded by the Ministry of SMEs and Startups (MSS, Korea.)

This paper is an extension of a conference paper, "High-speed Target SOC Alignment Algorithm for Second-life Battery Pack Maintenance." 2022 IEEE Transportation Electrification Conference & Expo (ITEC). IEEE, 2022, which is listed in [1].

Nguyen-Anh Nguyen, and Phuong-Ha La are with Department of Electrical, Electronic and Computer Engineering, University of Ulsan, Ulsan, South Korea (e-mail: nnanh1995@gmail.com and laphuongha@gmail.com).

Sung-Jin Choi is with Department of Electrical, Electronic and Computer Engineering, University of Ulsan, Ulsan, South Korea (e-mail: sjchoi@ulsan.ac.kr).

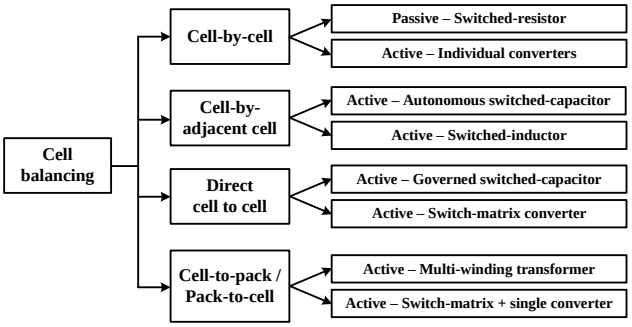

Fig. 1: Classification of the cell balancing methods in terms of equalization strategy.

equalization, equalization speed, and safety. Depending on the switch-matrix structure and the converter topology, the energy can be transferred from the battery pack to the cell (P2C) or cell to pack (C2P) [18], [19].

Another important feature lacking in detailed analysis is the target SOC freedom. In battery shipping and maintenance applications, the SOC of the battery pack is required to be topped up or released to an allowable level. In the swapping station, the cells inside a battery pack are equalized, and the whole pack is charged to a preset level and placed on standby for use as a replacement [20]–[22]. Or, if an EV has an issue on the road, the roadside service can transport a battery pack to the field for replacement. To ensure safe handling, the SOC level of the battery pack must be discharged under 30 % to achieve ready-to-ship status, according to the logistics safety policy [23], [24] and charged back to a nominal SOC level before being replaced in the swapping station. In addition, the SOC levels of all cells should be aligned to a specific target level. From the customer service perspective, during the charging process, the cells must be well equalized within a reasonable processing time [25]. Thus, an effective high-speed SOC alignment method is required.

In this paper, a novel SOC alignment algorithm is proposed to address the issue. The proposed algorithm, which is called the full-duplex coordinated strategy, utilizes a bidirectional pack-charger and cell-equalizer in a coordinated way to achieve the following advantages:

- To gain the freedom in SOC alignment.
- To minimize the switching pattern to reduce the energy loss.
- To minimize the processing time.

The remaining of this paper is organized as follows. The system configuration and half-duplex charge transfer strategy is reviewed and the full-duplex coordinated strategy for the SOC alignment process is proposed in Section II. Next, the theoretical analysis and process time optimization is provided in Section III. The performance of the proposed method is verified by the hardware experiments in Section IV. Finally, the conclusion is drawn in Section V.

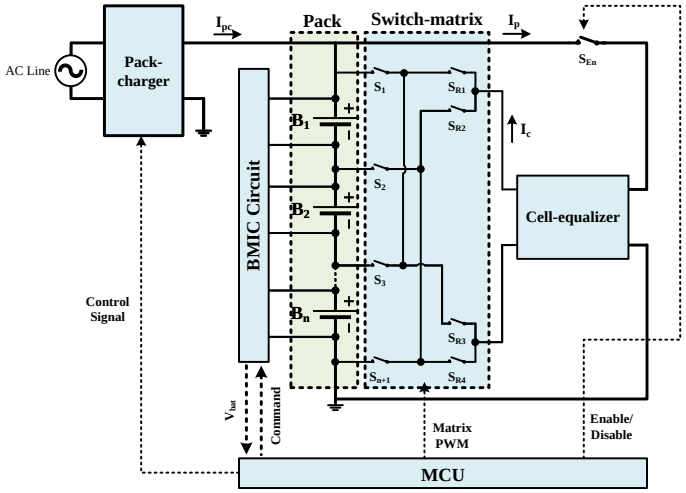

Fig. 2: Battery SOC alignment system.

II. SOC ALIGNMENT CONCEPT AND SYSTEM DESCRIPTION

A. System Configuration

This section describes the topological configuration and operation principle of the proposed SOC alignment system architecture. The main idea of the SOC alignment is to transfer energy from the high SOC cells to the low SOC cells until all cells are equalized. From an effectiveness perspective, the individual converter method, which uses a converter for each cell, is preferable. However, due to the additional cost and volume of this method, industrial sites are hesitant to adopt this approach. To reduce the cost, a switch-matrix is combined with a converter to charge or discharge one cell at a time for the equalization [16], [26]. Depending on the switch-matrix configuration, energy can be transferred from one cell to the other cell, from a cell to the pack, or from the pack to a cell. Since the cell-to-cell equalizer requires 4N number of switches (where N is the number of cells), the cell-to-pack or pack-to-cell methods have more practical feasibility.

Based on the main idea, the SOC alignment strategy is implemented in the topological configuration shown in Fig. 2. To minimize the number of switches in the matrix, the odd-even configuration is adopted. For N number of cells, the structure only requires N+5 number of switches, including N+1 number of switches (S_1 to S_{N+1}) for the equalization bus, and four switches (S_{R1}, S_{R2}, S_{R3}, S_{R4}) for the polarity inversion of cells. For instance, S_{R1} and S_{R4} are turned on if the odd-th cell is selected, while S_{R2} and S_{R3} are activated if the even-th cell is selected. In this paper, relays are used for the switches since isolation is naturally achieved and the cell voltages are monitored by the battery monitoring integrated circuit (BMIC). The cell OCVs are measured and used to estimate the SOC levels of the cells, which will decide the switching pattern of the switch-matrix and control algorithm for the cell-equalizer.

B. Conventional Charge Transfer Algorithm

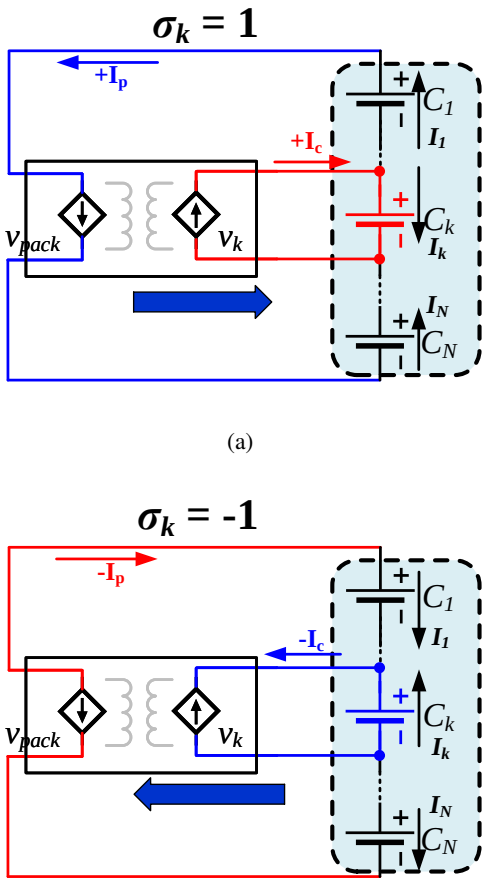

Fig. 3: Switching pattern of the switch-matrix: (a) Pack-to-cell mode; (b) Cell-to-pack mode.

1) Half-duplex Charge Transfer Algorithm: As mentioned above, any isolated converter and control strategy can be implemented with the switch-matrix. Fig. 3 illustrates the charge transfer during alignment. In the pack-to-cell mode, the cell-equalizer is controlled to charge the low SOC cell from the energy of the pack as shown in Fig. 3a. Whereas, in the cell-to-pack mode, the high SOC cell is discharged by the cell-equalizer and energy is transferred to the battery pack as shown in Fig. 3b. The conventional charge transfer strategy can achieve SOC alignment by utilizing a unidirectional isolated converter as shown in [27]. By charging the low SOC cells one by one with a specific individual processing time for each cell, energy is only transferred unidirectionally either in the pack-to-cell or cell-topack mode. Because of the unidirectional current flow in the cell equalizer, this method is called the half-duplex strategy.

At first, the initial SOC levels of the cells are estimated based on the initial cell voltages from the BMIC. Next, the cells are identified in ascending or descending order in terms of the SOC levels. The theoretical analysis in [27] provides the equations to calculate the processing times for every cell, which are used for the alignment process. Finally, the switch

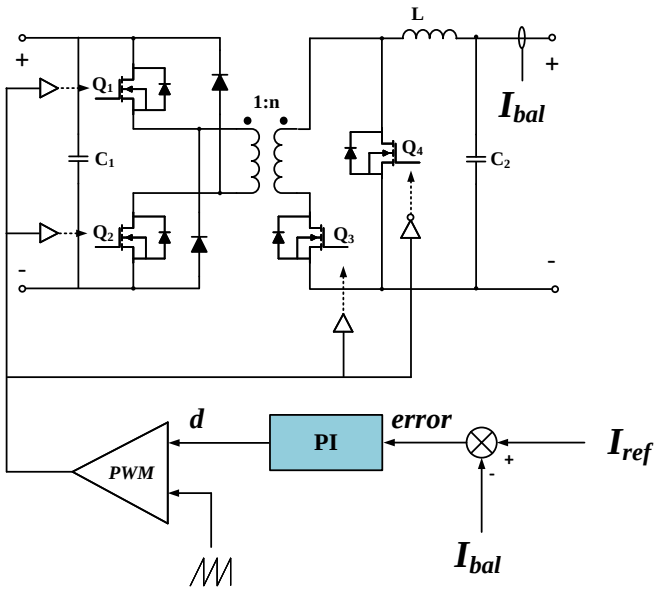

Fig. 4: Topology configuration of the cell-equalizer

pattern and processing time for every cell are performed one by one. However, the total alignment processing time is long and energy loss during the alignment is high.

2) Conventional Full-duplex Method: Another conventional bidirectional equalization method called the full-duplex max-min method [28], is used to compare with the proposed algorithm. However, because the processing time of the conventional method is not pre-calculated, but is determined by measurement and comparison, the SOC alignment process is not coordinated with the equalization. Therefore, the alignment operation has to be applied right after finishing the equalization.

The algorithm flow is as follows: In the beginning, the BMIC measures the cell OCVs and estimates the SOC of each cell. By measurement, the maximum, the minimum, and the average SOC levels are determined. In the next step, if the SOC difference between the maximum and the average SOC level is larger than a threshold, the maximum cell is discharged until the SOC difference becomes lower than the threshold value. After that, it changes the minimum SOC cell to reach the average SOC level. Then the process is repeated until the SOC difference between the maximum and the minimum cells are equal. After the balancing process, the SOC of the pack is re-estimated and the alignment operation is applied to adjust the SOC for reaching the target level.

C. Proposed Charge Transfer Algorithm

To increase the processing speed, the the full-duplex coordinated strategy is introduced. In this paper, the main idea is to allow the transfer of energy in a bidirectional way; the high SOC level cell is discharged to the pack, and the low energy SOC cell is charged from the pack. To reduce the cost and volume, a bidirectional topology is utilized. In this paper, a two-switch forward converter in Fig. 4 is chosen . The forward converter is designed based on the actual cell number and it can charge or discharge the cells by a constant current with a

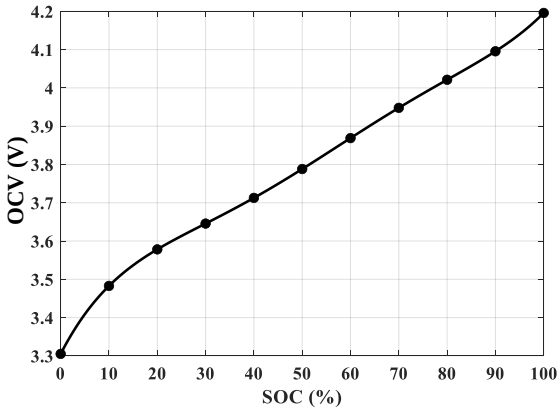

Fig. 5: SOC-OCV relationship.

PI controller. This topology is chosen due to its advantages of high transformer utilization, low peak current in both primary and secondary sides, less voltage stress. The detailed operation strategy will be discussed in the next section.

III. Operation Strategy and Process Time Optimization

A. Pack-charger Operation Strategy

The bidirectional pack-charger transfers the energy between the battery pack and the external power source based on the target SOC level. When the target SOC level is higher than the initial pack SOC level, the battery pack is charged. Whereas, if the target SOC level is lower than the initial pack SOC level, the battery pack is discharged by the pack-charger. Since the charging/discharging current level is usually fixed to the battery C-rate, the direction of the energy flow and the processing time are decided by the amount of the charge transfer. To determine the processing time required for the energy transfer process, the available capacity of a battery cell, Q_k, is defined as

$$Q_k(t) = SOC_k(t) Q_{M_k} \tag{1}$$

where k is the index of the battery cell, Q_{M_k} is the maximum capacity when the cell is fully charged, and SOC_k is the state of charge of the cell. Among various SOC estimation methods [29]–[38], this paper adopts the SOC-OCV method obtained in the ambient temperature of 25 ^oC. Under the different temperature condition, other SOC estimation methods with higher accuracy can be applied, then the effect of temperature on OCV can be considered. Fig. 5 describes the relationship between SOC and OCV (open-circuit voltage) of the battery cell, where the OCV can be calculated from the function of SOC, $f(SOC)$, based on the curve fitting method. Therefore, the initial $SOC_k(t_0)$ can be determined as

$$SOC_k(t_0) = f^{-1}[OCV_k(t_0)] \tag{2}$$

where $OCV(t_0)$ is the measured OCV of a cell at t_0 and f^{-1} is the inverse function of f. Accordingly, the initial average SOC of the battery pack, $SOC_{avg}(t_0)$, which is calculated by

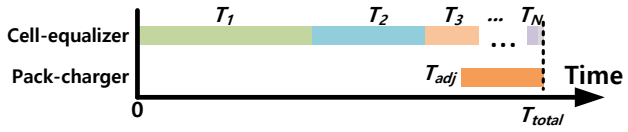

Fig. 6: Coordinated operation of SOC alignment concept over time.

the average value of the initial SOC of every cell, is expressed as

$$SOC_{avg}(t_0) = \frac{1}{N} \sum_{k=1}^{N} SOC_k(t_0) \tag{3}$$

where N is the total number of cells in the pack. In this paper, by applying the constant current (CC) method, the SOC level of the k^{th} cell is calculated as

$$SOC_k(t) = SOC_k(t_0) + \frac{I_k T_k}{Q_{M_k}} \tag{4}$$

where I_k is the charging current and T_k is the charging process period and is calculated as $T_k = t - t_0$. Therefore, for the given pack-charge current, I_{adj}, the required time for the SOC alignment, T_{adj}, to reach the targeted SOC level, SOC_{final}, is determined by

$$T_{adj} = \frac{[SOC_{final} - SOC_{avg}(t_0)] Q_{M_k}}{I_{adj}} \tag{5}$$

Notice that if T_{adj} is negative, the pack-charger should be operated in discharging mode.

B. Cell-equalizer Operation Strategy

In this section, the formula relating to the operation of the cell-equalizer and pack-charger during the SOC alignment process is theoretically analyzed. Assuming that the conversion efficiency of the cell-equalizer η, and the ratio of vc to vp is almost constant then current of battery pack, I_p, is almost constant and is determined as

$$I_p = \frac{1}{\eta} \frac{v_c I_c}{v_p} \tag{6}$$

where I_c is the magnitude of cell current generated by the cell-equalizer passing through one battery cell, v_c and v_p are the individual cell and pack voltage. Accordingly, equations are derived to calculate the processing time for every cells. For the cell-equalizer operation, because the charge transfer algorithm considers the bi-directional current flow, the analysis is based on the polarity convention in Fig. 3: the cell equalizer current flows from the pack to cell during the charging process, while it flows from the cell to pack during the discharging process. To describe the direction of the cell equalizer current for the k^{th} cell in a convenient way, the sign term is separated from the magnitude of the current and denoted as σ_k, then it can be expressed as

$$\sigma_k = \begin{cases} 1 & \text{pack-to-cell mode} \\ -1 & \text{cell-to-pack mode} \end{cases} \tag{7}$$

The cell current passing through the k^{th} cell, I_k, which is shown in Fig. 3 is determined as

$$I_k = \sigma_k (I_c - I_p). \tag{8}$$

Meanwhile, the current passing through the remaining cells is the pack current, which is calculated as

$$I_j = \sigma_k I_p \ (j = 1, 2, 3, ... \ and \ j \neq k). \tag{9}$$

During the SOC alignment process, the N steps of the operation is required. In each step, only one cell is activated by the switch-matrix. Therefore, the k^{th} cell is charged only in the time duration T_k, which is defined as the step time for the k^{th} cell, and discharged in the remaining time of processing. Hence, the SOC change during the process of the k^{th} cell is calculated by

$$SOC_k(t) - SOC_k(t_0) = \frac{\sigma_k I_c T_k}{Q_{M_k}} - \sum_{j=1}^{N} \frac{\sigma_j I_p T_j}{Q_{M_k}} \tag{10}$$

where T_k is the charging time of the k^{th} cell, T_j is the charging time of the others, and SOC_k is the SOC of the k^{th} cell. From (10), the step time of each cell multiplied by the current sign element, $\sigma_k T_k$, is calculated as

$$\sigma_k T_k = \frac{1}{I_c} \left\{ \left[SOC_k(t) - SOC_k(t_0) \right] Q_{M_k} + I_p \sum_{j=1}^{N} \sigma_j T_j \right\}. \tag{11}$$

The processing time, including loss of SOC per cell, T_k, is calculated as

$$T_k = |\sigma_k T_k|. \tag{12}$$

Finally, the total processing time of SOC alignment, T_{total}, is determined as

$$T_{total} = \sum_{k=1}^{N} T_k. \tag{13}$$

C. Processing Time Optimization

To optimize the total processing time, T_{total}, an optimization parameter is introduced as

$$W = \sum_{j=1}^{N} \sigma_j T_j. \tag{14}$$

Then the individual processing time is rewritten in terms of W as follows

$$T_k = \left| \frac{\left[SOC_k(t) - SOC_k(t_0) \right] Q_{M_k} + I_p W}{I_c} \right|. \tag{15}$$

As can be seen from (15), the processing time is dependent on W. By selecting the optimal value of W, the total processing time, T_{total}, can be minimized, where there always exists a value of W that makes the total processing time minimum. To find the minimum value, the derivative of T_{total} with respect to W is presented as

$$\frac{dT_{total}}{dW} = \sum_{k=1}^{N} \frac{dT_k}{dW} = \frac{I_p}{I_c} \sum_{k=1}^{N} \frac{\sigma_k T_k}{|\sigma_k T_k|} > 0. \tag{16}$$

Since it is a the non-zero positive number, the derivative of T_{total} is also larger than zero. Therefore, the T_{total} has the minimum value if W is one of the solutions of the derivative equation equal to 0. The parameter, W, at the minimum is expressed as

$$W = -\frac{\left[SOC_k(t) - SOC_k(t_0) \right] Q_{M_k}}{I_p} \quad (k = 1, 2, ..., N). \tag{17}$$

However, it is difficult to calculate the minimum point without further information. This situation can be mitigated by the median value calculation. If the median position is defined as

$$Med = \begin{cases} \frac{N+1}{2}, & \text{if } N \text{ is odd} \\ \frac{N}{2}, & \text{if } N \text{ is even} \end{cases} \tag{18}$$

the Cauchy-Schwartz inequality shows the total processing time, T_{total}, is optimized when W = W_{Med}, and W_{Med} is calculated as

$$W_{Med} = -\frac{\left[SOC_k(t) - SOC_k(t_0) \right] Q_{M_k}}{I_p} \quad (k = Med). \tag{19}$$

D. SOC Loss Compensation

In practical situation, the converter power loss results in the decline of SOC and it should be considered in the processing time calculation. The SOC loss of the battery pack can be determined as

$$SOC_L = \left(\frac{1}{\eta} - 1 \right) \frac{I_c}{N} \sum_{k=1}^{N} \frac{T_k}{Q_{M_k}} \tag{20}$$

where η is the conversion efficiency of the cell equalization. To compensate the SOC loss during the process, the SOC alignment time from (5) is re-calculated as

$$T_{adj} = \frac{\left[SOC_{final} - (SOC_{avg}(t_0) - SOC_L) \right] Q_{M_k}}{I_{adj}}. \tag{21}$$

Fig. 6 shows the overall coordinated operation of the SOC alignment over time. Both the pack-charger and cell-equalizer are controlled until the end of the process, and the cells are eventually aligned to the targeted SOC level. While the cell-equalizer processing time is assigned from T_1 to T_N, the pack-charger processing time is located at the end of the process. The total processing time, T_{total}, can be optimized when W = W_{Med}.

IV. Experimental Results

A. Experimental Setup

To verify the theoretical analysis, an experimental set-up is shown in Fig. 7, where a battery pack consists of 20-series cells (INR 18650 Li-NiMnCoO$_2$). The system includes a bidirectional forward converter as the cell-equalizer, a switch-matrix relay, and BMICs (Analog Device, LTC6804-1). An offline bidirectional power supply is used as the pack-charger to charge or discharge the whole battery pack and the battery

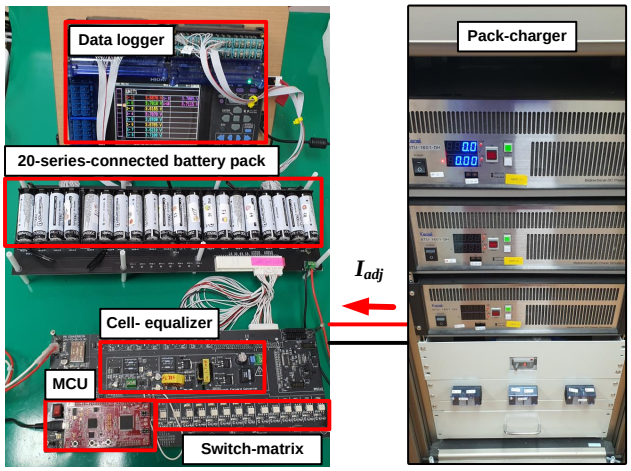

Fig. 7: Experimental setup.

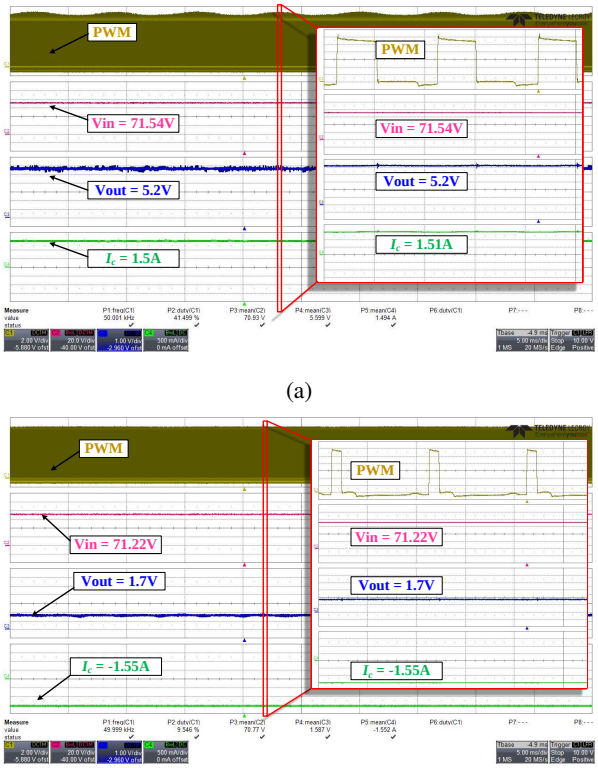

Fig. 8: Forward converter operation waveform: (a) Pack-to-cell mode; (b) Cell-to-pack mode.

cell voltages are logged by the data logger (Hioki LR8402). The experimental parameters include that the pack-charger current, I_{adj}, is set at 1A and the cell-equalizer current, I_c, is 1.5 A. The measured internal battery impedance, Z_b, is 0.01 Ω. Fig. 8 shows the waveform of the bidirectional forward converter implemented in two modes of operation: pack-to-cell and cell-to-pack. In Fig. 8a, the input voltage of the converter is measured at 71.54 V, the output voltage is 5.2 V, and the targeted cell is charged with 1.5 A in the pack-to-cell mode. Similarly, the targeted cell is discharged with

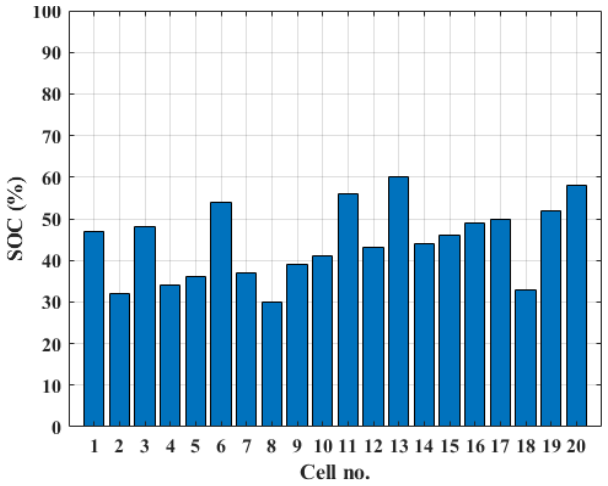

Fig. 9: Initial SOC conditions of 20-cell Lithium-ion battery (18650 - 3.6V/2.9A)

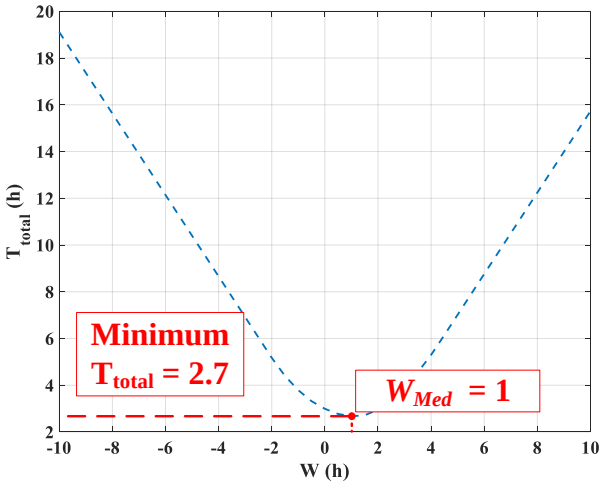

Fig. 10: Evaluation of the total processing time, T_{total}, versus the weighted sum of the processing time, W.

-1.5 A in the cell-to-pack mode as shown in Fig. 8b. In order to draw a comparison, both the conventional full-duplex strategy and the half-duplex strategy are implemented. Due to the unforeseen processing time associated with the full-duplex max-min method, the alignment operation is executed immediately upon completion of the equalization process. The time taken for the alignment operation is then calculated using equation (5).

Fig. 9 shows the initial SOC condition of the 20-cell batteries. The initial SOCs are randomly scattered from 30 % to 60 %. To investigate the dependency of T_{total} on W, the total processing time versus W is plotted in Fig. 10. It is noticed that the curves of T_{total} versus W are the concave functions, It is interesting to observe that a strong positive W prolongs the total processing time since the cell-equalizer tends to be operated in the unidirectional pack-to-cell mode. Likewise, a strong negative W also results in a longer total processing time, since the cell-equalizer is mostly operated in the unidirectional cell-to-pack mode. By the theoretical

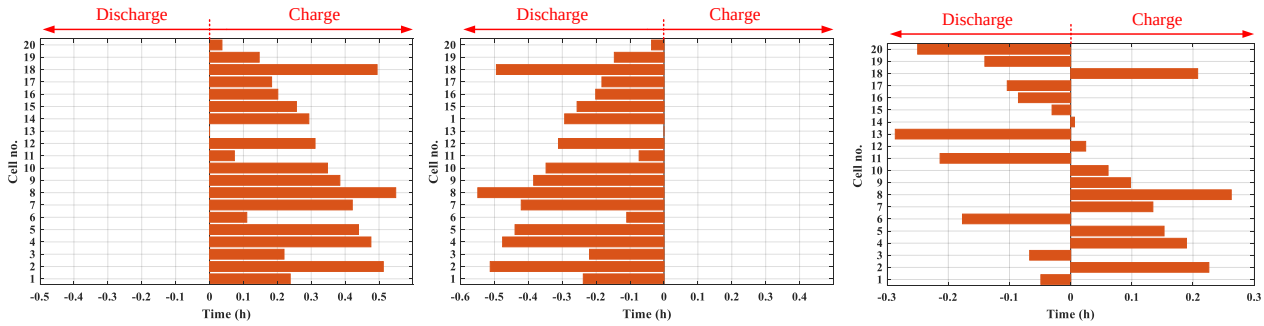

Fig. 11: Cell processing time map: (a) Pack-to-cell-only strategy wit $W = 5$; (b) Cell-to-pack-only strategy with $W = -3.4$; (c) Proposed strategy with $W = 1$.

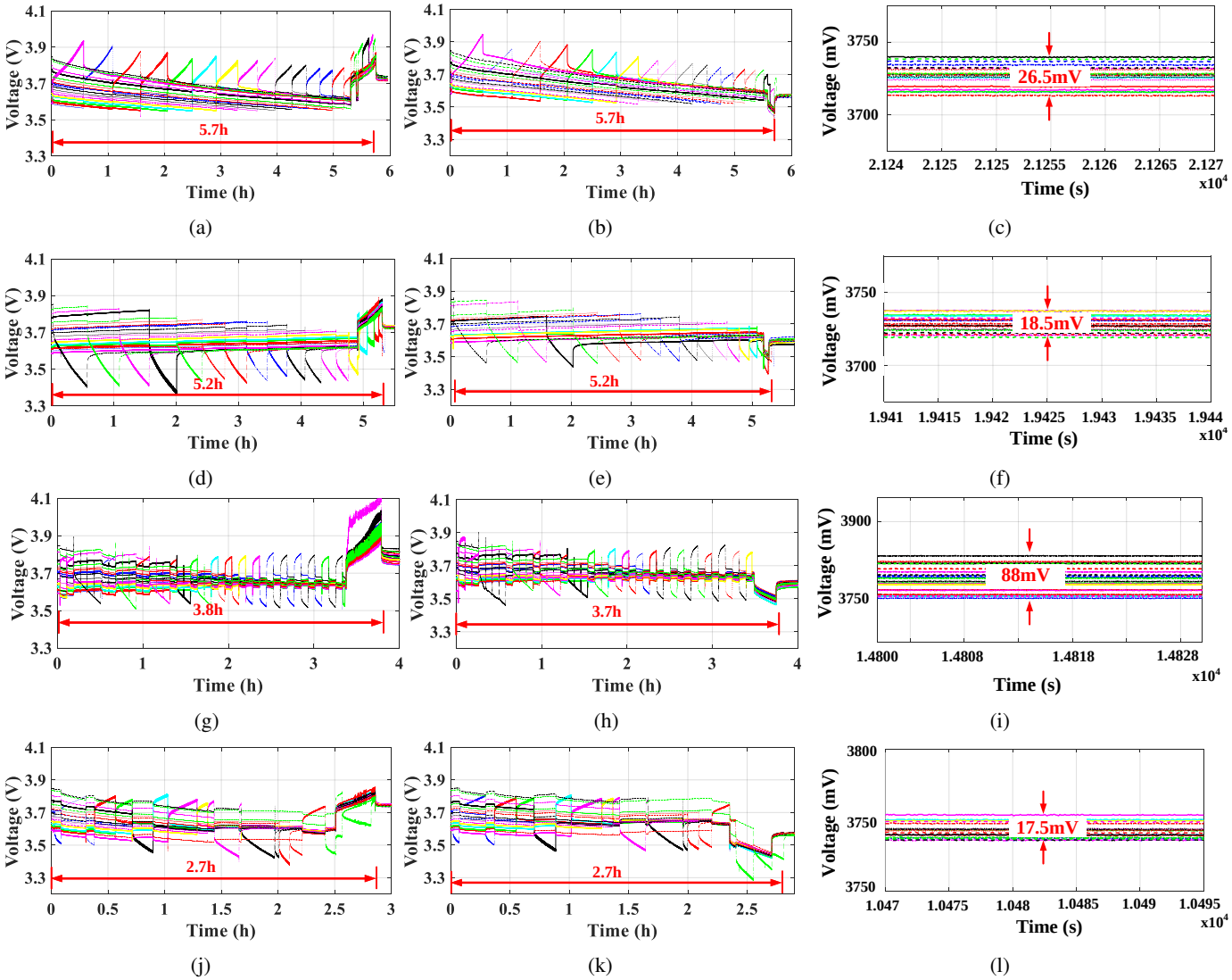

Fig. 12: Voltage profile at 55% SOC target, voltage profile at 30% SOC target, and the final voltage deviation with different strategies: (a)-(c) Pack-to-cell-only strategy; (d)-(f) Cell-to-pack-only strategy; (g)-(i) Max-min strategy; (j)-(l) Proposed strategy.

analysis, the T_{total} has the minimum value of 2.7h at $W = 1$ calculated from (19) and it will be verified by the experimental test in the following section.

Fig. 11 shows the cell processing time map of 20 series-connected cells according to the analyzed results of the

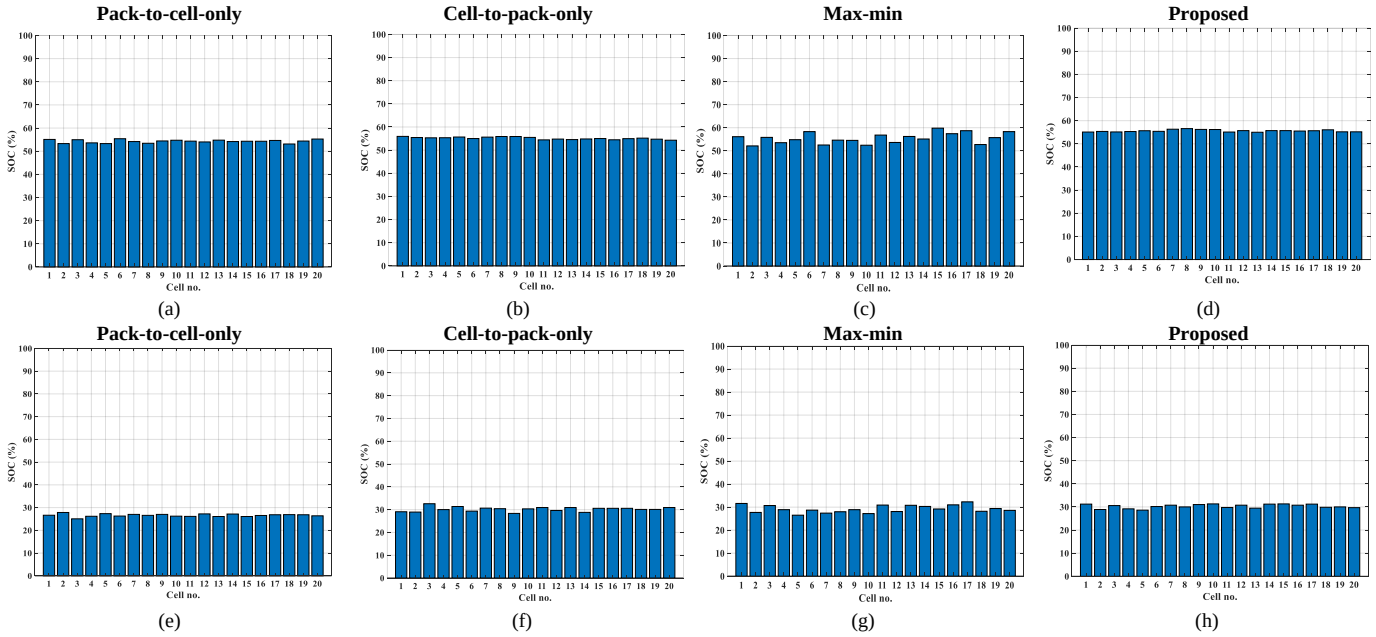

Fig. 13: SOC profile with pack-to-cell-only, cell-to-pack-only, max-min and proposed strategies: (a)-(d) 55% SOC target; (e)-(h) 30% SOC target.

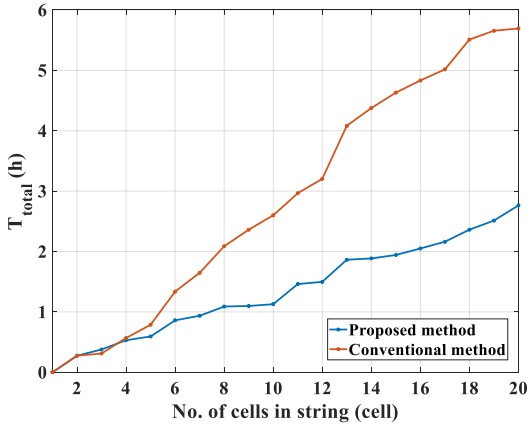

Fig. 14: Total processing time comparison between two strategies with different number of cells.

conventional and proposed strategy. The step time of half-duplex strategy is determined in pack-to-cell-only and cell-to-pack-only strategies, which represents the conventional strategy [27], while the step time of the full-duplex strategy is calculated based on (15) and (19). Note that a positive T_k demonstrates the pack-to-cell energy transfer direction, and a negative T_k represents the cell-to-pack energy transfer direction. Fig. 11a analyzes the step time to transfer the energy from pack-to-cell by the half-duplex strategy. The time index shows that the longest operation time for one cell is over 1.5 hours. Fig. 11b shows the additional scenario of the half-duplex strategy in the cell-to-pack-only strategy, where the cell is discharged and the energy is transferred to the pack. In both half-duplex scenarios, the total processing time is about 5.7 hours. However, in Fig. 11c, the time index analyzed by the proposed strategy ($W = 1$) shows a significant reduction in the step time duration, where the longest step time is only 0.3 hours and the total processing time is about 2.7 hours.

B. SOC Alignment Process

Fig. 12 shows the experimental results to compare the performance of the half-duplex strategy and the full-duplex strategy. The voltage profiles of the SOC alignment go with their voltage deviations and are demonstrated in several strategies with the target set at 55 % and 30 %. Fig. 12a to 12c show the SOC alignment processes in pack-to-cell-only strategy, where the total processing time to balance and achieve the targeted SOC is 5.7 hours with a voltage deviation of 26.5 mV. As can be seen from the results in Fig. 12d to 12f, the SOC alignment process in cell-to-pack-only strategy requires the total processing time of 5.2 hours to reach a 28.5 mV voltage deviation. Fig. 12g to 12i show the SOC alignment processes in the full-duplex max-min strategy, where the total processing time to balance and achieve the targeted SOC is 3.7 hours with a voltage deviation of 88 mV. In Fig. 12g, even though the cells are balanced, the voltage deviation becomes worse after applying the alignment process due to the different cell characteristics. It is concluded that the uncoordinated operation between the pack-charger and cell-equalizer can lead to another imbalanced condition. Compared to the conventional strategies, the processing time by the proposed full-duplex coordinated strategy only needs 2.7 hours to complete the SOC alignment process as shown in Fig. 12j to 12l. Therefore, the proposed strategy achieves 47 %, 52 %, and 28.9 % faster processing duration compared to the conventional strategies

Fig. 13 shows the final SOC level of the conventional and proposed strategy. Figs. 13a to 13d show the final SOC profiles of the targeted SOC at 55 %. In these figures, the SOC errors

TABLE I: Test results

Strategy	SOC Target	Processing time	Final voltage deviation	Final SOC deviation	SOC Loss	Energy loss
Pack-to-cell-only	30%	$5.7h$	$23.0mV$	2.8%	15.3%	$0.1938Wh$
	55%	$5.7h$	$26.5mV$	4.3%	15.3%	$0.1938Wh$
Cell-to-pack-only	30%	$5.2h$	$27.5mV$	4.2%	13.6%	$0.1879Wh$
	55%	$5.2h$	$18.5mV$	2.0%	13.6%	$0.1879Wh$
Bidirectional Max-min	30%	$3.7h$	$41.0mV$	5.8%	5.4%	$0.1347Wh$
	55%	$3.8h$	$88.0mV$	7.7%	4.8%	$0.1633Wh$
Proposed strategy	30%	$2.7h$	$17.0mV$	1.7%	4.5%	$0.1206Wh$
	55%	$2.7h$	$17.5mV$	1.6%	4.5%	$0.1206Wh$

of the conventional and proposed strategies are 4.3 %, 2.0 %, 7.7 %, and 1.6 %, respectively. Similarly, Figs. 13e to 13h illustrate the final SOC profiles of the conventional strategies and the proposed strategy with the SOC target at 30 %. Their SOC errors are 2.8 %, 4.2 %, 5.8 %, and 1.7 %, respectively. The results demonstrate that the proposed strategy can achieve the targeted SOC level of the battery pack with an error of less than 3 % and get better performance than the conventional strategies.

C. Voltage, SOC Deviation, and Energy Loss of Batteries

Minimizing the processing time also helps to reduce energy loss. The energy loss inside the battery, generated during the total processing time, is calculated based on the operation of the pack-charger and the cell-equalizer as

$$E_{loss} = NZ_b(I_{adj} - I_p)^2 T_{adj} + NZ_b I_p^2 (T_{total} - T_{adj}) + Z_b I_c^2 T_{total} \quad (22)$$

where Z_b is the internal resistance of one cell.

The results in TABLE I demonstrate that the proposed strategy reduces SOC loss by 70 %, and the processing time is twice as fast as the half-duplex strategy. The proposed strategy has a lower energy loss of 36 % and 38 % when compared to the conventional half-duplex strategies of 0.1938 Wh and 0.1879 Wh, respectively. Compared to the conventional full-duplex max-min method, the proposed method shows similar SOC loss, but it can save 12.2 % and 26.1 % of energy during the process for two target SOC levels of 30 % and 50 %, respectively. Therefore, the proposed strategy with an optimal processing time is advantageous in saving energy.

In Fig. 14, the total processing time of the conventional method and the proposed method is compared with a different number of cells. When the number of cells is small ($N < 5$), the total processing time is almost similar; however, when the number of cells becomes larger, the processing time deviation increases significantly. The trend shows that the processing time of the proposed method can be up to three hours faster than the conventional method with 20 cells in series. Therefore, with a hundred cells in the battery pack, the proposed method becomes substantially effective in the SOC alignment process.

V. Conclusion

This paper proposes a novel high-speed SOC alignment system for series-connected battery pack. With the SOC alignment architecture including the pack-charger and cell-equalizer, the full-duplex charge-transfer algorithm is presented and the optimization process is provided. Compared to the conventional strategy, the experimental results verified the high performance of the proposed strategy. The proposed strategy can save 52 % and 28.9 % of the processing time, while reducing energy loss by 38 %, 10.4 % and 26.1 % compared to the conventional strategies. To conclude, the proposed hardware architecture and the control strategy is suitable for the EV battery maintenance purpose.

References

[1] N.-A. Nguyen, P.-H. La, and S.-J. Choi, "High-speed target soc alignment algorithm for second-life battery pack maintenance," in *2022 IEEE Transportation Electrification Conference & Expo (ITEC)*, pp. 131–136. IEEE, 2022.

[2] U. S. A. B. Consortium *et al.*, "Usabc electric vehicle battery test procedure manual, rev. 2," 1996.

[3] I. E. Agency. Global ev outlook 2020. [Accessed July 26, 2020]. [Online]. Available: https://webstore.iea.org/global-ev-outlook-2020"

[4] M. Weil and S. Ziemann, "Recycling of traction batteries as a challenge and chance for future lithium availability," in *Lithium-Ion Batteries*, pp. 509–528. Elsevier, 2014.

[5] T. R. Hawkins, B. Singh, G. Majeau-Bettez, and A. H. Strømman, "Comparative environmental life cycle assessment of conventional and electric vehicles," *Journal of industrial ecology*, vol. 17, no. 1, pp. 53–64, 2013.

[6] Z. Song, S. Feng, L. Zhang, Z. Hu, X. Hu, and R. Yao, "Economy analysis of second-life battery in wind power systems considering battery degradation in dynamic processes: Real case scenarios," *Applied Energy*, vol. 251, p. 113411, 2019.

[7] E. Martinez-Laserna, I. Gandiaga, E. Sarasketa-Zabala, J. Badeda, D.-I. Stroe, M. Swierczynski, and A. Goikoetxea, "Battery second life: Hype, hope or reality? a critical review of the state of the art," *Renewable and Sustainable Energy Reviews*, vol. 93, pp. 701–718, 2018.

[8] C. Herrmann, A. Raatz, S. Andrew, and J. Schmitt, "Scenario-based development of disassembly systems for automotive lithium ion battery systems," in *Advanced Materials Research*, vol. 907, pp. 391–401. Trans Tech Publ, 2014.

[9] Y. Zheng, M. Ouyang, L. Lu, and J. Li, "Understanding aging mechanisms in lithium-ion battery packs: From cell capacity loss to pack capacity evolution," *Journal of Power Sources*, vol. 278, pp. 287–295, 2015.

[10] I. Baghdadi, O. Briat, J.-Y. Delétage, P. Gyan, and J.-M. Vinassa, "Lithium battery aging model based on dakin's degradation approach," *Journal of Power Sources*, vol. 325, pp. 273–285, 2016.

[11] S. F. Schuster, T. Bach, E. Fleder, J. Müller, M. Brand, G. Sextl, and A. Jossen, "Nonlinear aging characteristics of lithium-ion cells under different operational conditions," *Journal of Energy Storage*, vol. 1, pp. 44–53, 2015.
[12] M.-Y. Kim, C.-H. Kim, J.-H. Kim, and G.-W. Moon, "A chain structure of switched capacitor for improved cell balancing speed of lithium-ion batteries," *IEEE Transactions on Industrial Electronics*, vol. 61, no. 8, pp. 3989–3999, 2013.
[13] A. C. Baughman and M. Ferdowsi, "Double-tiered switched-capacitor battery charge equalization technique," *IEEE Transactions on Industrial Electronics*, vol. 55, no. 6, pp. 2277–2285, 2008.
[14] M.-Y. Kim, J.-H. Kim, and G.-W. Moon, "Center-cell concentration structure of a cell-to-cell balancing circuit with a reduced number of switches," *IEEE Transactions on Power Electronics*, vol. 29, no. 10, pp. 5285–5297, 2013.
[15] T. H. Phung, A. Collet, and J.-C. Crebier, "An optimized topology for next-to-next balancing of series-connected lithium-ion cells," *IEEE transactions on power electronics*, vol. 29, no. 9, pp. 4603–4613, 2013.
[16] P.-H. La and S.-J. Choi, "Direct cell-to-cell equalizer for series battery string using switch-matrix single-capacitor equalizer and optimal pairing algorithm," *IEEE Transactions on Power Electronics*, vol. 37, DOI 10.1109/TPEL.2022.3147842, no. 7, pp. 8625–8639, 2022.
[17] Y. Shang, Q. Zhang, N. Cui, B. Duan, Z. Zhou, and C. Zhang, "Multicell-to-multicell equalizers based on matrix and half-bridge lc converters for series-connected battery strings," *IEEE Journal of Emerging and Selected Topics in Power Electronics*, vol. 8, DOI 10.1109/JESTPE.2019.2893167, no. 2, pp. 1755–1766, 2020.
[18] M. Raeber, A. Heinzelmann, and D. O. Abdeslam, "Analysis of an active charge balancing method based on a single nonisolated dc/dc converter," *IEEE Transactions on Industrial Electronics*, vol. 68, DOI 10.1109/TIE.2020.2972449, no. 3, pp. 2257–2265, 2021.
[19] S.-W. Lee, Y.-G. Choi, and B. Kang, "Active charge equalizer of li-ion battery cells using double energy carriers," *Energies*, vol. 12, no. 12, p. 2290, 2019.
[20] F. Ahmad, M. Saad Alam, I. Saad Alsaidan, and S. M. Shariff, "Battery swapping station for electric vehicles: opportunities and challenges," *IET Smart Grid*, vol. 3, no. 3, pp. 280–286, 2020.
[21] Y. Zheng, Z. Y. Dong, Y. Xu, K. Meng, J. H. Zhao, and J. Qiu, "Electric vehicle battery charging/swap stations in distribution systems: comparison study and optimal planning," *IEEE transactions on Power Systems*, vol. 29, no. 1, pp. 221–229, 2013.
[22] W. Zhan, Z. Wang, L. Zhang, P. Liu, D. Cui, and D. G. Dorrell, "A review of siting, sizing, optimal scheduling, and cost-benefit analysis for battery swapping stations," *Energy*, p. 124723, 2022.
[23] H. Huo, Y. Xing, M. Pecht, B. J. Züger, N. Khare, and A. Vezzini, "Safety requirements for transportation of lithium batteries," *Energies*, vol. 10, no. 6, p. 793, 2017.
[24] I. A. T. Association, "Shipping lithium batteries - transporting lithium batteries by air, sea and road," 2020.
[25] R. Guo, L. Lu, M. Ouyang, and X. Feng, "Mechanism of the entire overdischarge process and overdischarge-induced internal short circuit in lithium-ion batteries," *Scientific reports*, vol. 6, p. 30248, 2016.
[26] S. Yarlagadda, T. T. Hartley, and I. Husain, "A battery management system using an active charge equalization technique based on a dc/dc converter topology," *IEEE Transactions on Industry Applications*, vol. 49, no. 6, pp. 2720–2729, 2013.
[27] N.-A. Nguyen, P.-H. La, and S.-J. Choi, "Coordinated operation algorithm of pack-chargers and cell-equalizers for soc adjustment in second-life batteries," *Journal of Power Electronics*, vol. 22, no. 1, pp. 105–115, 2022.
[28] M. A. Hannan, M. M. Hoque, S. E. Peng, and M. N. Uddin, "Lithium-ion battery charge equalization algorithm for electric vehicle applications," *IEEE Transactions on Industry Applications*, vol. 53, no. 3, pp. 2541–2549, 2017.
[29] J. Meng, M. Ricco, G. Luo, M. Swierczynski, D.-I. Stroe, A.-I. Stroe, and R. Teodorescu, "An overview and comparison of online implementable soc estimation methods for lithium-ion battery," *IEEE Transactions on Industry Applications*, vol. 54, no. 2, pp. 1583–1591, 2017.
[30] K. S. Ng, C.-S. Moo, Y.-P. Chen, and Y.-C. Hsieh, "Enhanced coulomb counting method for estimating state-of-charge and state-of-health of lithium-ion batteries," *Applied energy*, vol. 86, no. 9, pp. 1506–1511, 2009.
[31] Y.-M. Jeong, Y.-K. Cho, J.-H. Ahn, S.-H. Ryu, and B.-K. Lee, "Enhanced coulomb counting method with adaptive soc reset time for estimating ocv," in *2014 IEEE Energy Conversion Congress and Exposition (ECCE)*, pp. 1313–1318. IEEE, 2014.
[32] M. A. Varnosfaderani and D. Strickland, "Online impedance spectroscopy estimation of a battery," in *2016 18th European Conference on Power Electronics and Applications (EPE'16 ECCE Europe)*, pp. 1–10. IEEE, 2016.
[33] J. A. A. Qahouq and Z. Xia, "Single-perturbation-cycle online battery impedance spectrum measurement method with closed-loop control of power converter," *IEEE Transactions on Industrial Electronics*, vol. 64, no. 9, pp. 7019–7029, 2017.
[34] Y.-M. Jeong, Y.-K. Cho, J.-H. Ahn, S.-H. Ryu, and B.-K. Lee, "Enhanced coulomb counting method with adaptive soc reset time for estimating ocv," in *2014 IEEE Energy Conversion Congress and Exposition (ECCE)*, pp. 1313–1318. IEEE, 2014.
[35] S. Tong, M. P. Klein, and J. W. Park, "On-line optimization of battery open circuit voltage for improved state-of-charge and state-of-health estimation," *Journal of Power Sources*, vol. 293, pp. 416–428, 2015.
[36] M. Cacciato, G. Nobile, G. Scarcella, and G. Scelba, "Real-time model-based estimation of soc and soh for energy storage systems," *IEEE Transactions on Power Electronics*, vol. 32, no. 1, pp. 794–803, 2016.
[37] J. Xu, C. C. Mi, B. Cao, J. Deng, Z. Chen, and S. Li, "The state of charge estimation of lithium-ion batteries based on a proportional-integral observer," *IEEE Transactions on Vehicular Technology*, vol. 63, no. 4, pp. 1614–1621, 2013.
[38] N.-A. Nguyen, P.-H. La, and S.-J. Choi, "Pre-heating method employing pulse current excitation for effective charging of lib in low-temperature environment," in *2023 11th International Conference on Power Electronics and ECCE Asia (ICPE 2023-ECCE Asia)*, pp. 2125–2131. IEEE, 2023.

Nguyen-Anh Nguyen comes from Ho Chi Minh City, Vietnam. He received his B.S. degree in Physics from the Ho Chi Minh University of Science, Ho Chi Minh City, Vietnam, in 2017. After graduating, he worked as a Software Engineer at Robert Bosch Engineering Vietnam, Ho Chi Minh City, Vietnam, from 2017 to 2019. Since 2020, he has been working towards his Ph.D. degree in the Energy Conversion Circuit Laboratory, University of Ulsan, Ulsan, South Korea. His current research interests include battery management systems, battery chargers, and cell balancing.

Phuong-Ha La received a B.S. degree in Automation and Control Systems from the University of Technology - National University of Ho Chi Minh City in 2014. He completed his M.s. & Ph.D. Degrees in Power Electronics from the University of Ulsan in February 2023. From 2013 to 2017, he worked for Dien Quang Lamp JSC. as an R&D and project management specialist. Since March 2023, he has been a Principal Value Engineer at Pepperl-Fuchs Vietnam. His research interests include battery management systems, battery chargers, cell balancing circuits, symbiosis equalizing-state estimating systems, and sensor systems.

Sung-Jin Choi received his B.S., M.S., and Ph.D. degrees in Electrical Engineering from Seoul National University, Seoul, South Korea, in 1996, 1998, and 2006, respectively. From 2006 to 2008, he was a Research Engineer with Palabs Company Ltd., Seoul, South Korea. From 2008 to 2011, he was the Principal Research Engineer with Samsung Electronics Company Ltd., Suwon, South Korea, where he was responsible for developing LED drive circuits and wireless battery charging systems. In 2011, he joined the University of Ulsan, Ulsan, South Korea, where he is presently working as Professor in the Department of Electrical, Electronic and Computer Engineering. He was a Visiting Scholar at San Diego State University, San Diego, CA, USA from 2017 to 2018 and at University of Colorado Denver, Denver, CO, USA in 2022. Dr. Choi is the Editor of the Journal of Power Electronics. His current research interests include modeling and control of high-frequency power converters in solar power generation, battery management, and wireless power transfer.